

Article

Control Strategy for Building Air Conditioning Cluster Loads Participating in Demand Response Based on Cyber-Physical System

Xiaoling Yuan ^{1,*}, Hao Cao ², Zheng Chen ³, Jieyan Xu ³ and Haoming Liu ²

¹ College of Artificial Intelligence and Automation, Hohai University, Nanjing 211100, China

² College of Energy and Electrical Engineering, Hohai University, Nanjing 211100, China; hcao@hhu.edu.cn (H.C.); liuhaom@hhu.edu.cn (H.L.)

³ State Grid (Beijing) Integrated Energy Planning and D&R Institute, Beijing 100052, China; chenzheng0302@126.com (Z.C.); powerxjy@vip.163.com (J.X.)

* Correspondence: lingx@hhu.edu.cn

Abstract: In recent years, with rising urbanization and ongoing adjustments in industrial structures, there has been a growing dependence on public buildings. The load of public buildings gradually becomes the main component of the peak load in summer, among which the load of air conditioning is particularly prominent. To clarify the key problems and solutions to these challenges, this study proposes a multi-objective optimization control strategy for building air conditioning cluster participation in demand response based on Cyber-Physical System (CPS) architecture. In a three-layer typical CPS architecture, the unit level of the CPS achieves dynamic information perception of air conditioning clusters through smart energy terminals. An air conditioning load model based on the multiple parameter types of air conditioning compressors is presented. Then, the system level of the CPS fuses multiple pieces of information through smart energy gateways, analyzing the potential for air conditioning clusters when they participate in demand response. The system of system level (SoS level) of the CPS deploys a multi-objective optimization control strategy which includes the uncertainty of the initial states of air conditioning clusters within the intelligent building energy management system. The optimal model takes into account the differences in the environmental conditions of each individual air conditioning unit within the cluster and sets different operating modes for each unit to achieve load reduction while maintaining temperatures within a comfortable range for the human body. The Multi-Objective Particle Swarm Optimization (MOPSO) algorithm based on Pareto frontiers is applied to solve this optimization control strategy and to optimize the operational parameters of the air conditioning clusters. A comparative analysis is conducted with single-objective optimization results obtained using the traditional Particle Swarm Optimization (PSO) algorithm. The case study results indicate that the proposed multi-objective optimization control strategy can effectively improve the thermal comfort of the human body towards the controlled temperatures of air conditioning clusters while meeting the accuracy of demand response. In the solution phase, the highest temperature within the air conditioning clusters is 24 °C and the lowest temperature is 23 °C. Adopting the proposed multi-objective optimization control strategy, the highest temperature is 26 °C and the lowest temperature is 23.5 °C within the clusters and the accuracy of demand response is up to 92%. Compared to the traditional PSO algorithm, the MOPSO algorithm has advantages in convergence and optimization precision for solving the proposed multi-objective optimization control strategy.

Keywords: Cyber-Physical System; air conditioning clusters; demand response; pareto front; MOPSO



Citation: Yuan, X.; Cao, H.; Chen, Z.; Xu, J.; Liu, H. Control Strategy for Building Air Conditioning Cluster Loads Participating in Demand Response Based on Cyber-Physical System. *Energies* **2024**, *17*, 1291. <https://doi.org/10.3390/en17061291>

Academic Editor: Boris Igor Palella

Received: 1 February 2024

Revised: 28 February 2024

Accepted: 5 March 2024

Published: 7 March 2024



Copyright: © 2024 by the authors. Licensee MDPI, Basel, Switzerland. This article is an open access article distributed under the terms and conditions of the Creative Commons Attribution (CC BY) license (<https://creativecommons.org/licenses/by/4.0/>).

1. Introduction

In recent years, with rising urbanization and ongoing adjustments in industrial structures, there has been a growing dependence on public buildings. Building energy con-

sumption now accounts for over 30% of total energy consumption. This trend reflects the evolving landscape of urban development and industrial shifts, with a particular spotlight on the energy consumption issue of air conditioning [1]. In China, the rapid increase in air conditioning load during the summer places significant pressure on the safe operation of the power grid, with 30–40% of the peak load being in summer and up to 50% being in first-tier cities such as Beijing and Shanghai [2]. The increased air conditioning load in summer leads to periodic adjustments in the power system, resulting in insufficient peak capacity of the power grid [3]. A 2018 report from the International Energy Agency (IEA) predicts that by 2050, the global energy consumption of air conditioning will be equivalent to China's current total demand for electricity [4]. Increases in the installed capacity on the generation side for short-term peak loads may lead to problems such as overcapacity, low unit utilization, and resource wastage. As demand-side and grid-side two-way interaction capabilities continue to rise, demand-side resources are becoming an important resource for grid dispatching operations, which can effectively promote the transformation of the grid mode. Nowadays, the smart grid consists of multiple power sources and loads with wide spatial and temporal distribution. The flexible change in load serves as a major means to balance power fluctuations.

Therefore, building loads exert a significant impact on the secure, stable, and economical operation of the power grid. It is urgent to explore the untapped energy efficiency potential of buildings, achieve efficient utilization of an entire building's energy through the integration of information flow and energy flow, integrate building energy services with grid regulation, and promptly create comprehensive energy services for public buildings as well as ensure efficient interaction with the upper-level power grid. This strategy will function as a key focus for the development of the power industry.

Currently, an increasing number of studies focus on decentralized air conditioning loads used in residential or small commercial buildings [5–9]. The equivalent thermal parameter (ETP) model, based on circuit simulation, and the building model, based on heat and cold load calculations, are commonly used to simulate heat storage [10]. The ETP model includes outdoor temperature, building environment, indoor heat and cold sources, and temperature with relevant circuit parameters such as capacitance, reactance, and resistance. It simulates the heat exchange process between the interior of the room and the exterior by modeling the equivalent parameters of the circuit. Zhang et al. (2014) [11] developed a third-order model considering the temperature variability of the inner and outer walls. Bashash and Fathy (2013) [12] utilized a second-order simplified model that overlooks the difference between the inner and outer walls for convenience.

The widely used air conditioning control method is direct load control (DLC) [13], which includes start-stop control [14], gear control [15], and cyclic wheel stop control [16]. Other control methods have also been extended and developed. Wang et al. (2019) [17] proposed a semi-Markov process-based probabilistic control method for air conditioning loads, with the air conditioning system divided into four states: on, off, on-locked, and off-locked. Tian et al. (2019) [18] applied the state-space model to the air conditioning wheel control method. In addition to direct load control, model predictive control (MPC) has been the focus of current research [19]. Mr. Joe and Mr. Karava (2019) [20] used the MPC model to regulate heating and cooling systems in office buildings to maintain comfortable indoor temperatures. Vedullapalli et al. (2019) [21] proposed an MPC-based model for HVAC combined with building energy storage to participate in demand response.

Metaheuristic algorithms are a class of methods based on computational intelligence mechanisms employed to identify optimal solutions to complex optimization problems. Also referred to as intelligent optimization algorithms, these methods effectively tackle nonlinear optimization problems and handle multi-constraint scenarios. With the development of computer networks and artificial intelligence technology, metaheuristic algorithms are increasingly applied to the formulation of control strategies for air conditioning. Li et al. (2017) [22] presented a non-dominated sorting-based particle swarm optimization (NSPSO) algorithm, together with the Kriging method, for the optimization of the HVAC system de-

sign in a typical office room. Chiuhsiang Joe Lin et al. (2022) [23] proposed a multi-objective optimization model based on the multi-objective whale optimization algorithm to balance energy consumption and thermal comfort in air conditioning and mechanical ventilation systems. The regulation of water flow rate, air volume, and indoor air temperature reduced energy consumption. Siyuan Y. et al. (2023) [24] suggested an improved parallel artificial immune system algorithm to ascertain the optimal operational parameters of the system under varying loads, with the aim for the maximization of operational efficiency.

In summary, existing control strategies for individual air conditioning systems participating in demand response have developed numerous mature theories. However, research on air conditioning clusters participating in demand response is relatively scarce. Additionally, in many studies on the CPS, most have proposed localized optimization for energy systems. An overall analysis shows that these studies lack global perception and collaboration, making it difficult to achieve overall energy optimization at the system level.

Therefore, this paper proposes a control strategy for the participation of building air conditioning clusters in demand response, based on CPS architecture and considering the construction requirements of the energy internet, along with the operational characteristics of air conditioning clusters in the building sector. This approach is important for improving the stability of the power grid. The innovative points of this study are as follows:

(1) At the unit level of the CPS, an air conditioning load model based on the multiple parameter types of air conditioning compressors was established.

(2) At the system level of the CPS, the potential of air conditioning clusters participation in demand response was analyzed. The operating status of air conditioning in different environments was simulated by changing the equivalent heat capacity and equivalent thermal resistance of each room. The set temperature of the air conditioning cluster was changed and the results were analyzed.

(3) At the SoS level of the CPS, a multi-objective optimization control strategy was proposed to address the air conditioning clusters. The control strategy was developed by the uncertainty of the initial states of air conditioning clusters, the ETP model, and the human-thermal-comfort model. The control strategy concluded the differences in the environmental conditions of each individual air conditioning unit within the cluster and changed the set temperature every 15 min for each air conditioning unit to achieve load reduction while maintaining the temperature of each room to meet the demand of human body thermal comfort.

(4) The Multi-Objective Particle Swarm Optimization (MOPSO) algorithm based on the Pareto front was used to solve this optimization control strategy and optimize the operational parameters of the air conditioning clusters. A comparative analysis was conducted with single-objective optimization results obtained using the traditional Particle Swarm Optimization (PSO) algorithm. The case study showed that compared to the PSO algorithm, the MOPSO algorithm has the advantages of strong convergence and global search ability when solving the multi-objective control strategy proposed in this paper.

2. System Concept and the Architecture Analysis of the CPS

2.1. System Concept of CPS

A CPS is a system that integrates computer science with physical processes, enabling real-time data exchange, automation control, and intelligent algorithms to monitor, analyze, and control the physical world [25]. CPSs play a crucial role in improving system efficiency, security, and reliability and are widely applied in industries, transportation, healthcare, and other fields. Applying CPSs to building energy systems in both energy supply and demand sides leverages their reliable perception and precise control features to provide real-time sensing of the physical environment within buildings. This enables the control of air conditioning clusters based on the actual environmental conditions, ultimately achieving the goal of “maximizing supply, minimizing consumption, and optimizing comfort”. The typical architecture of CPSs consists of three layers: unit level, system level, and SoS level.

The unit level of the CPS is the smallest unit of the information-physical system. It forms a data closed-loop of “perception-analysis-decision-execution” through smart energy terminals, each of which is an identifiable and connected information carrier. The unit-level CPS, through industrial networks, enables broader and more extensive automatic data flow, leading to the establishment of smart production lines, smart workshops, and smart factories, facilitating the interconnection, interoperability, and communication of multiple unit-level CPSs, further enhancing the breadth, depth, and precision of manufacturing resource optimization.

The system level of the CPS combines intelligent energy gateways and energy management systems through industrial networks, enabling even greater automatic data flow in a broader range and wider domains, connecting and intercommunicating multiple unit-level CPSs. The system level of the CPS is based on the state perception, information exchange, and real-time analysis of multiple unit-level CPS minimum units, achieving energy efficiency analysis, energy efficiency diagnosis, and coordinated control of multiple devices in buildings. The system level of the CPS includes the Building Energy Management System (BEMS), the Home Energy Management System (HEMS), and the Enterprise Energy Management System (EEMS).

The BEMS integrates building automation systems, energy management systems, and building management systems, into a comprehensive system. The BEMS centrally monitors, manages, and controls the energy usage status of a building or building clusters’ electrical distribution, lighting, elevators, air conditioning, heating, water supply, and drainage, etc., providing hardware and software systems for the online monitoring and dynamic analysis of building energy consumption.

The HEMS connects various devices in homes (such as audiovisual equipment, lighting systems, curtain control, air conditioning control, security systems, digital cinema systems, media servers, audio cabinet systems, networked appliances, etc.) through Internet of Things technology, offering various functions and means such as home appliance control, lighting control, remote control via phone, indoor and outdoor remote control, anti-theft alarm, environmental monitoring, HVAC control, infrared forwarding, and programmable timing control.

The EEMS comprehensively applies intelligent management systems to achieve efficient integration of human and machine elements in enterprise management and to realize “human-machine coordination” in enterprises.

The system of system level (SoS level) of the CPS is an organic combination of multiple system-level CPSs, encompassing four key elements: “hardware, software, network, and platform” [26]. It mainly includes the central station of the intelligent building management system and sub-stations for load aggregation. Through a big data platform, the SoS-level CPS achieves interconnection, interoperability, and communication across systems and platforms, facilitating the integrated exchange and sharing of data from various sources. This closed-loop automatic flow allows for comprehensive information perception, in-depth analysis, scientific decision-making, and precise execution on a global scale. The platform-level CPS, through the intelligent electricity main station system, aggregates and optimizes the energy response potential of multiple commercial buildings.

2.2. The System Architecture of the CPS

In this paper, the type of public building is an office building with 50 rooms. Figure 1 shows a diagram of a multi-level control system of the CPS for the air conditioning clusters of this public building.

The unit level depicts individual air conditioning units in various rooms, with sensors and controllers for each unit. It demonstrates how data are collected and commands are transmitted, representing the control loop at the most granular level.

The system level shows the platform of the BEMS, detailing its functions such as state perception, real-time analysis, and coordinated control of equipment. It also in-

cludes the evaluation of human thermal comfort and the calculation of Demand Response (DR) accuracy.

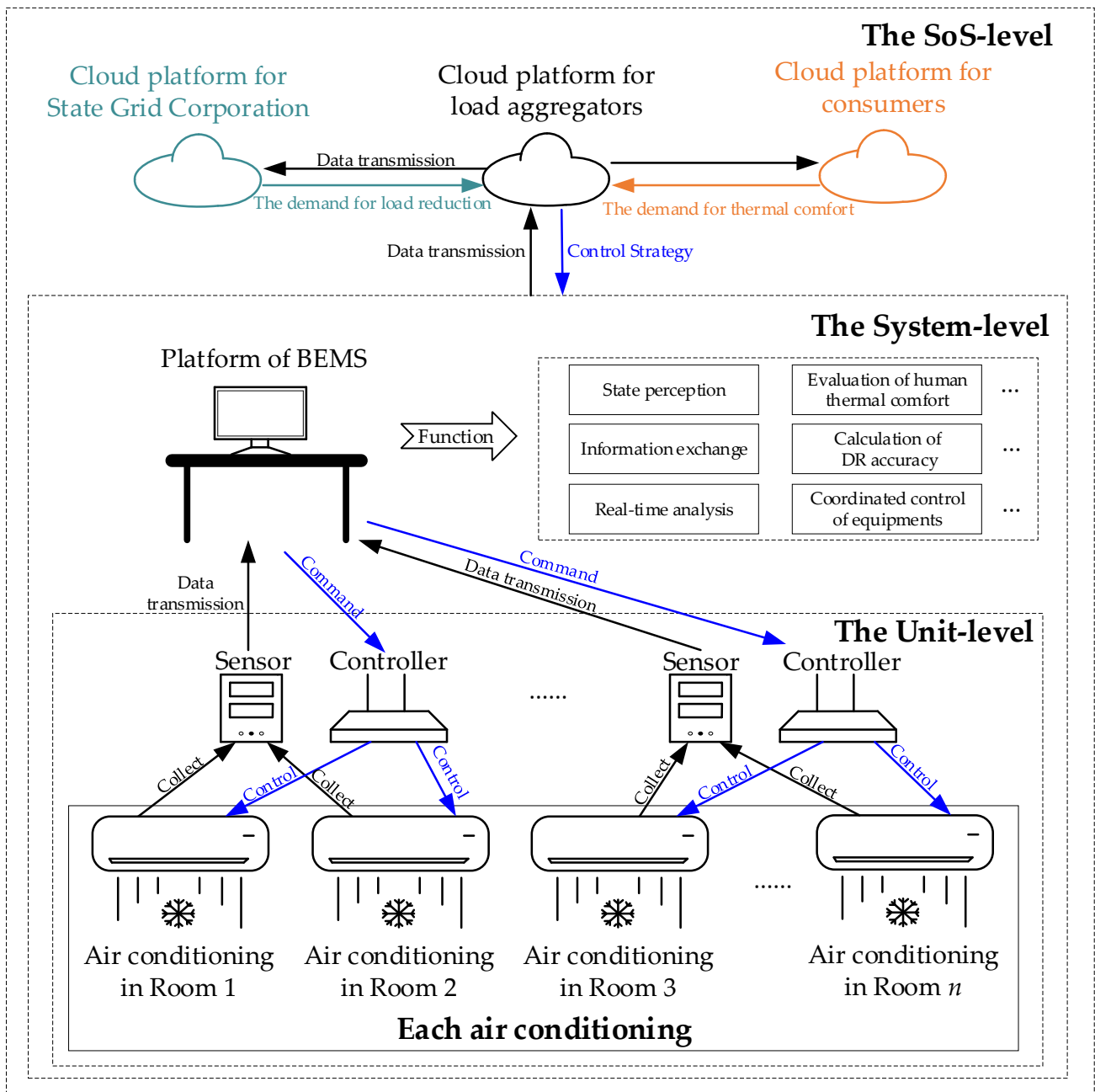


Figure 1. A diagram of a multi-level control system of the CPS for the air conditioning clusters.

The SoS level illustrates the data exchange between different cloud platforms, highlighting the data transmission pathways from the State Grid Corporation, load aggregators, and consumers. It shows the demand for thermal comfort and the demand for load reduction and thermal comfort. Then, the platform of load aggregators formulates control strategies for air conditioning clusters.

The multi-level control system of the CPS proposed in this study enables differentiated control of air conditioning clusters, bearing significant practical implications. Intelligent energy management, especially for high-consumption air conditioning systems, can substantially enhance energy efficiency and reduce operational costs, offering considerable economic benefits to commercial building managers. On another note, dynamically control-

ling air conditioning clusters based on real-time data and user demands, while ensuring human comfort, plays a crucial role in improving the satisfaction and experience of building occupants. The application and dissemination of such technologies serve as a model for energy management and environmental protection in smart city development, contributing to the overall advancement of urban intelligence.

3. The Unit Level of the CPS

At the unit level of the CPS, mathematical models are developed based on the physical properties and operational principles of air conditioning, translating these physical processes into mathematical equations. These models range from simple linear equations to complex differential equations, capturing the fundamental dynamics of each unit. Furthermore, the parameters of the mathematical models are estimated based on experimental data or the literature. This step ensures an accurate representation of the actual behavior of air conditioning, utilizing the models to simulate the behavior of units and the entire system under different scenarios. Such simulations aid in optimizing the performance, energy efficiency, and safety of the CPS.

3.1. ETP Model

The rapid increase in air conditioning loads during the summer has exacerbated the supply–demand imbalance in urban power grids. The regulation of air conditioning loads through demand-side management can alleviate pressure on the grid during peak loads. However, due to the diverse types of air conditioning loads which have their different operational characteristics, the construction of a reasonable air conditioning load model becomes essential for more effective participation of air conditioning loads in power system scheduling.

The ETP model is commonly used in research for modeling air conditioning loads. Its principle involves the initial conversion of relevant data, such as indoor temperature, outdoor ambient temperature, and air conditioning cooling/heating capacity, into equivalent electrical circuit components. This conversion enables the use of an equivalent circuit to simulate the heat exchange process between the indoor and outdoor environments.

The first-order ETP model is as Equation (1) [1]

$$\frac{dT_{in}}{dt} = \frac{1}{RC}(T_{out} - T_{in}) - \frac{Q_t}{C} \quad (1)$$

$$Q_t = \eta \cdot P_t \quad (2)$$

where T_{in} is the indoor temperature at time t ; T_{out} is the outdoor temperature at time t ; R and C refer to the equivalent thermal resistance and equivalent heat capacity, respectively; Q_t is the cooling capacity at time t ; η is the energy efficiency ratio of the air conditioning system; and P_t is the power of the air conditioning system. The differential equation governing the indoor temperature variation in the building has been established, which serves as the basis for the derivation of the time-varying equation for indoor temperature.

3.2. Air Conditioning Load Model Based on the Frequency of the Compressor

An air conditioning load model based on air conditioning compressor frequency was studied in the literature [27]. This study involved varying frequencies of variable-frequency air conditioning while maintaining constant indoor and outdoor conditions. The resulting simulation data were used to analyze the operating characteristics of the air conditioning system. Figure 2 shows the relationship between the refrigeration capacity and the energy efficiency ratio of the air conditioning system.

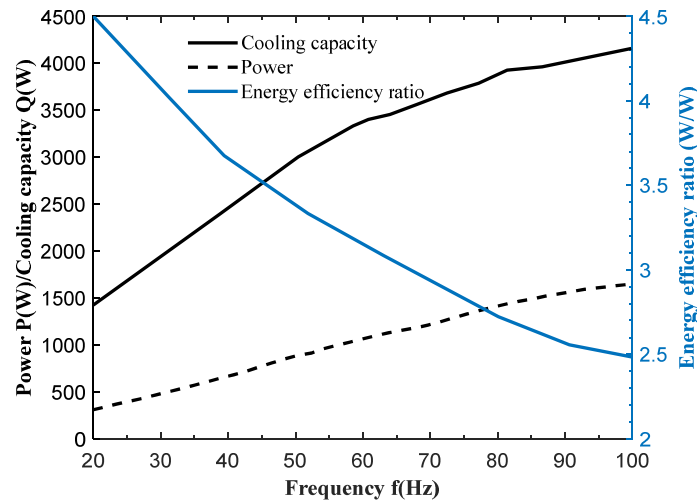


Figure 2. The relationship between the refrigeration capacity and the energy efficiency ratio.

According to Figure 2, the power P_t can be fitted as a first-order function as Equation (3), and the cooling capacity can be fitted as a second-order function as Equation (4)

$$P_t = a \cdot f_t + b \quad (3)$$

$$Q_t = c \cdot f_t^2 + d \cdot f_t + e \quad (4)$$

where f_t represents the frequency of the compressor of the air conditioning system at time t ; and a, b, c, d , and e represent constant coefficients of the respective functions.

The compressor frequency varies with the temperature difference between the indoor temperature and the set temperature [28]

$$\Delta T^t = T_{in}^t - T_{set}^t \quad (5)$$

$$f_{t+1} = \begin{cases} f_{\max} & \Delta T^t > M \\ f_t + \theta \cdot \Delta T & m \leq \Delta T^t \leq M \\ f_{\min} & \Delta T^t < m \end{cases} \quad (6)$$

$$f_{\min} \leq f_t \leq f_{\max} \quad (7)$$

$$T_{set,\min}^t \leq T_{set}^t \leq T_{set,\max}^t \quad (8)$$

where ΔT^t is the temperature difference between the indoor temperature and the set temperature; T_{set}^t is the set temperature at time t ; f_{\max} and f_{\min} represent the frequency up and down limits of the compressor respectively; and θ is a positive constant.

4. The System Level of the CPS

At the system level of the CPS, temperature, humidity, and other relevant data from each room in the building are gathered through sensors and smart devices. These data are then analyzed to assess the thermal characteristics of each room and the operational status of the air conditioning system. By considering variations between different rooms and their temperature requirements, the potential and accuracy of the air conditioning cluster's participation in demand response are calculated. Furthermore, utilizing collected environmental parameters and personnel information, the Predicted Mean Vote (PMV) model is employed to compute the PMV value for each room.

4.1. Thermal Comfort of Human Body

Thermal comfort refers to the subjective evaluation of the human body's satisfaction with the surrounding thermal environment. The PMV is used to evaluate the human comfort in this paper which is denoted as Equation (9) [29]

$$f_{PMV} = [0.303e^{-0.036M} + 0.0275] \times \{M - W - 3.05[5.73 - 0.007(M - W) - p_a] - 0.0014M(34 - t_a) - 0.0173M(5.87 - p_a) - 0.42(M - W - 58) - f_{cl}h_c(t_{cl} - t_a) - 3.96 \times 10^{-8}f_{cl}[(t_{cl} + 273)^4 - (t_r + 273)^4]\} \quad (9)$$

where M is metabolism; f_{cl} is the ratio of clothing and body surface area; t_{cl} is the average temperature of human body surface with clothing; t_r is the mean radiation temperature; P_a is the partial pressure of water vapor in the ambient air; t_a is the air temperature; h_c is the convective heat exchange coefficient; and W is the power of human body.

The PMV equation is a regression equation obtained by Fanger through experimental fitting of the relationship between heat load, metabolism, and PMV value. Table 1 provides the PMV thermal perception scale.

Table 1. PMV thermal feeling scale.

Sensation	Cold	Cool	Slightly Cool	Fit	Mild Warm	Warm	Hot
Value of PMV	−3	−2	−1	0	1	2	3

The Predicted Percentage Dissatisfied (PPD) indicates dissatisfaction with a hot environment, represented as Equation (10) [30].

$$f_{PPD} = 100 - 95e^{-(0.03353 f_{PMV}^4 + 0.21 f_{PMV}^2)} \quad (10)$$

The recommended PMV value for satisfying environmental thermal comfort falls within the range of $[-0.5, 0.5]$, and the corresponding PPD value in the interval is $[5\text{--}10\%]$.

4.2. Accuracy of the Demand Response Control Strategy

The aggregator receives the total reduction task from a power company and allocates tasks according to the potential assessment of air conditioning clusters. The power company disburses subsidies and imposes penalties based on the overall task completion of the aggregator. Consumers who have implemented power reductions according to a contract will be compensated by the aggregator. The aggregator's revenue is generally calculated based on the subsidies and penalties from the power company, and the cost reduction. Therefore, the accuracy of the demand response strategy is directly related to the revenue of the aggregator, as demonstrated in the following equation

$$w = 1 - \frac{\left| \sum_{n=1}^N P_{2,n}(t) - P_{tar} \right|}{P_{tar}} \quad (11)$$

where w defines the accuracy of the demand response control strategy. The closer w is to 1, the higher the accuracy of the demand response strategy.

5. The SoS Level of the CPS

The SoS level of the CPS facilitates interconnection, interoperability, and communication between systems and platforms, promoting the integrated exchange and sharing of data from various sources. The Load Aggregation Merchant Cloud Platform is responsible for coordinating and managing various subsystems within buildings, including the deployment of control strategies for air conditioning clusters.

5.1. Control Strategy for Air Conditioning Based on the Variation of Temperature

Load aggregators control the degree of load reduction as they change the set temperature of the air conditioning cluster based on the scheduling requirements of the power system. Figure 3 shows the relationship between the power of variable-frequency air conditioning and the indoor temperature.

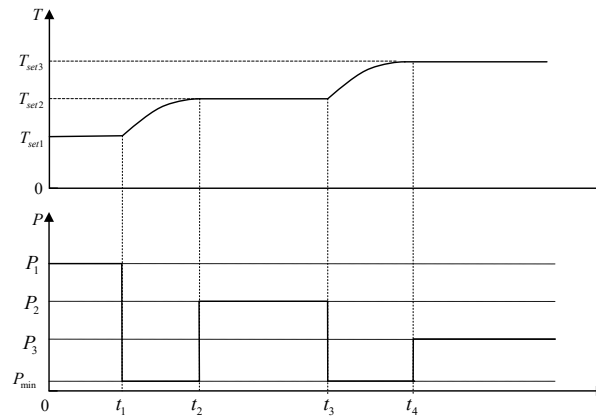


Figure 3. The relationship between power and the indoor temperature.

In Figure 3, T_{set1} , T_{set2} , and T_{set3} represent three different set temperatures, respectively, with $T_{set1} < T_{set2} < T_{set3}$. The corresponding air conditioning power is denoted as P_1 , P_2 , and P_3 , where $P_1 > P_2 > P_3$. Before time T_1 , the air conditioning system operates with the set temperature T_{set1} , and the power is P_1 . At time t_1 , the set temperature is changed to T_{set1} , and the air conditioning system operates at the lowest power P_{min} . When the indoor temperature reaches T_{set2} at time t_2 , the air conditioning power is changed to P_2 to maintain the temperature until the set temperature is changed to T_{set3} at time t_3 , and the air conditioning system's power is P_{min} .

5.2. Control Strategy for Air Conditioning Clusters Based on Load Aggregators and Consumers

This study proposes separate control functions for load aggregators and consumers.

5.2.1. Control Functions for Load Aggregators

The load aggregator changes the set temperature of the air conditioning clusters based on the scheduling requirements of the power system. The aim is to influence the operational state of the air conditioning clusters and control load reduction during demand response moments. Therefore, the first objective of this paper is to optimize the control of the set temperatures of individual variable-frequency air conditioning systems within the cluster, which seeks to minimize the deviation between the actual operation power and the target power of the variable-frequency air conditioning clusters, as demonstrated in the following equations

$$\min \sum o_1(t) \quad (12)$$

$$o_1(t) = \left| \sum_{n=1}^N P_{2,n}(t) - P_{tar} \right| \quad (13)$$

$$P_{tar} = \sum_{n=1}^N P_{1,n}(t) - D \quad (14)$$

where $o_1(t)$ is the deviation between the actual operation power and target power of the air conditioning clusters; $P_{2,n}(t)$ is the power of the n th air conditioning system at time t after participating in demand response; P_{tar} is the reduction power of the air conditioning clusters; $P_{1,n}(t)$ is the power of the n th air conditioning system at time t before participating

in demand response; and D is the trading volume after the clearing of the day-ahead market in the demand response conducted by the grid dispatch.

5.2.2. Control Functions for the Consumers

The control strategy minimizes the temperature difference in the set temperature before and after the regulation of the air conditioning clusters. The decision variable in this optimization is the set temperature after the control, as demonstrated in the following equations

$$\min \sum o_2(t) \tag{15}$$

$$f_{o_2}(t) = \sum_{n=1}^N \left(T_n^{set2}(t) - T_n^{set1}(t) \right)^2 \tag{16}$$

$$o_2(t) = \frac{\sqrt{f_{o_2}(t)}}{N} \tag{17}$$

$$T_{\min} \leq T_n^{set2} \leq T_{\max} \tag{18}$$

where $o_2(t)$ is the difference function in the temperature changes of the air conditioning clusters before and after the control; T_n^{set1} and T_n^{set2} are the temperatures set at time t before and after the n th air conditioning system participates in demand response; and T_{\min} and T_{\max} are the down and up limits of the set temperature.

5.3. The MOPSO Algorithm Based on the Pareto Optimal Solution

5.3.1. Pareto Optimal Solution

Pareto Optimality, also known as Pareto Efficiency, was proposed by Vilfredo Pareto, an Italian sociologist. This concept refers to an ideal state of resource allocation. Assuming a fixed number of individuals and a fixed pool of allocable resources, any change in the existing allocation status is considered a Pareto improvement or a Pareto optimality if it makes at least one individual better off without making anyone else worse off.

In the context of multi-objective optimization problems, the optimization of one objective based on intelligent algorithms may lead to the deterioration of other objectives due to potential conflicts among various optimization objectives. Consequently, there may be more than one optimal solution when solving such problems.

The set of all solutions within the Pareto optimal solution set, which is mapped in the objective space, forms a surface known as the Pareto Front. Figure 4 shows a distribution of the Pareto solution set. A and B are located in the objective space which represents the Pareto Front. The collection of all solutions on the Pareto Front is referred to as the Pareto optimal solution set. The solution to multi-objective optimization problems involves the identification of this non-dominated solution set.

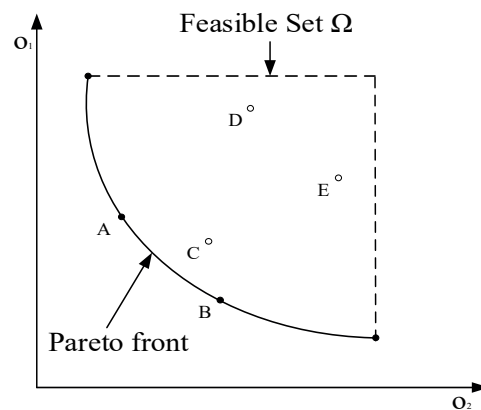


Figure 4. The diagram of the Pareto solution set.

5.3.2. MOPSO Algorithm

The MOPSO algorithm was proposed by Coello et al. in 2002 [31]. The specific steps of the MOPSO algorithm are as follows:

1. Set $t = 0$, randomly initialize the population P_t , calculate the objective function value vectors for each particle, and add the non-dominated solutions to the external archive (i.e., the set of non-dominated solutions obtained during each iteration), NP_t ;
2. Confirm the initial individual $p_i(0)$ and global best values $g_i(0)$ for each particle;
3. Update the particle positions and velocities to form the next generation of subpopulations while adjusting the individual best values $p_i(t)$ for each particle;
4. Use the new non-dominated solutions to maintain the external archive, generate the external archive for the next iteration, and determine the global best value $g_i(t)$ for each particle;
5. Let $t = t + 1$. If the termination condition of the algorithm is satisfied, end the search; otherwise, return to step 3.

In solving multi-objective optimization, different objective problems may have different global best values, with these different global best values non-dominated by each other. In other words, the global best value $g_i(t)$ is not unique in this case. Therefore, when the MOPSO algorithm is running, attention should be paid to the selection of individual best values, the maintenance of global best values, the management of the external archive, and ensuring particles fly within the feasible space. Figure 5 is the flowchart of the MOPSO algorithm.

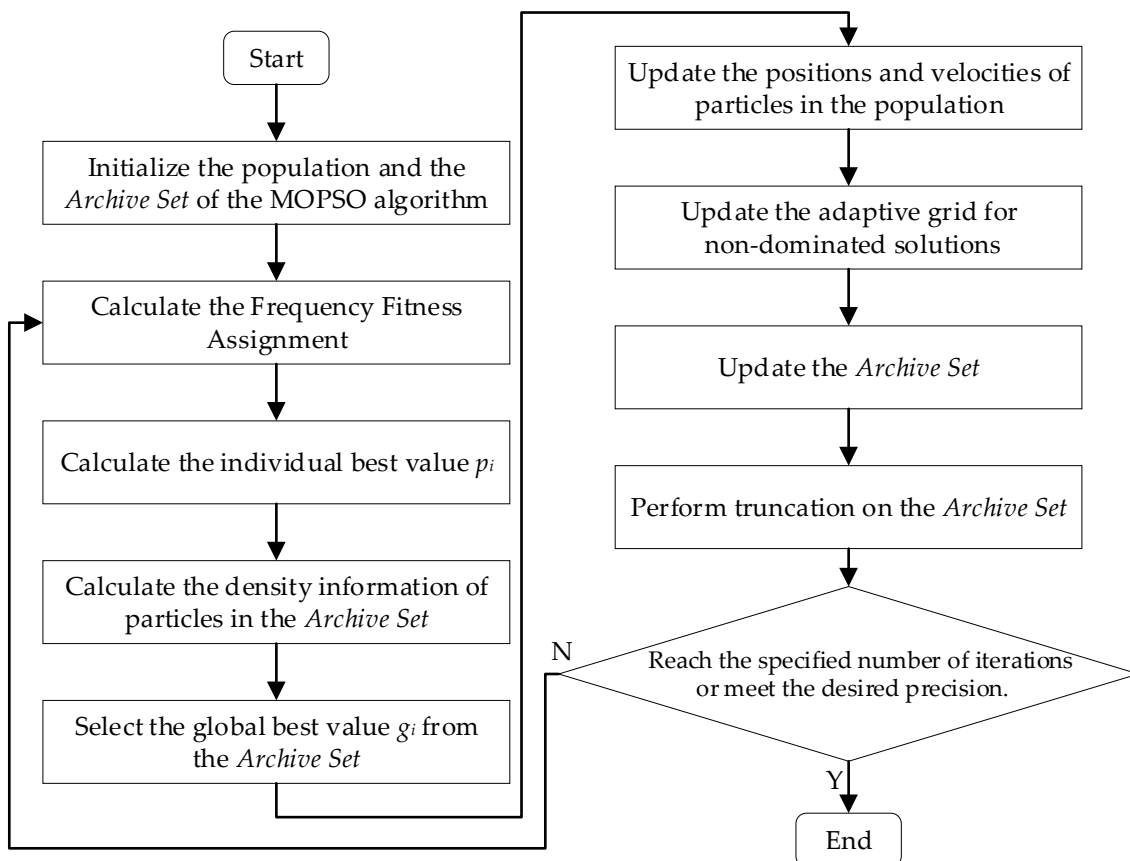


Figure 5. The flowchart of the MOPSO algorithm.

6. Case Study

6.1. Potential Assessment of Air Conditioning Clusters Participating in Demand Response

This study assumes that the type of public building is an office building with a BEMS, it has 50 rooms, and there is one variable-frequency air conditioning system in each room. These air conditioning systems come from the same brand and have a rated power of 1.8 kW. Therefore, the universal parameters for the air conditioning load model are established. However, due to each air conditioning system operating in different environmental conditions, a differentiated parameter configuration is applied to the ETP model, specifically for equivalent thermal capacitance and resistance. Such differentiation involves the diversity of the internal building environment, aiming to more accurately depict the operational characteristics of the air conditioning system in different spaces. Table 2 shows the parameters of this study case.

Table 2. The parameter settings of the case study.

Parameter	Value
$T_{out}/^{\circ}\text{C}$	35
$R/(^{\circ}\text{C}/\text{kW})$	R~N (10, 1)
$C/(\text{kJ}/^{\circ}\text{C})$	C~N (200, 0.5)
f_{min}/Hz	5
f_{max}/Hz	110
a	15.23
b	125
c	-0.1
d	60
e	200

6.1.1. The Temperature Changes of Each Room with the Same Set Temperature When the Initial Temperature Is the Same

By setting the parameters of the load model of variable-frequency air conditioning clusters systems based on the ETP model, the initial temperature of each room is the same, all at 28 °C. Taking the changing of the set temperature of the air conditioning clusters to 23 °C as an example, the result is as follows.

Figure 6 shows the temperature changes in each room where each air conditioning system is located in this scenario. The enlarged section in the figure indicates that the time required for each room to reach the target temperature varies. Meanwhile, the temperature of each room changes within a certain range of the set temperature due to the different operating states of their respective air conditioning systems.

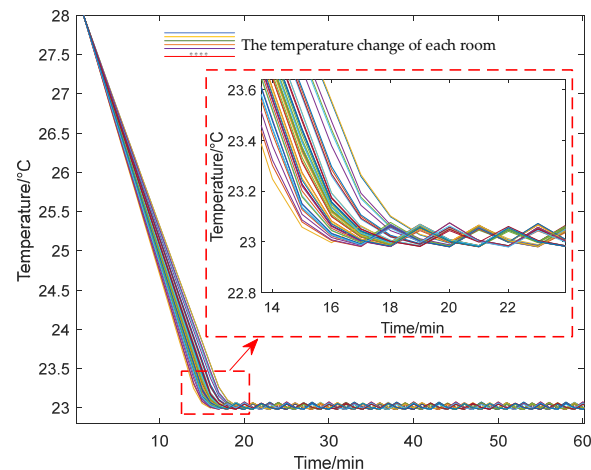


Figure 6. The temperature change of each room as the set temperature of the air conditioning clusters is 23 °C.

6.1.2. The Potential Analysis of Air Conditioning Clusters Participation in Demand Response under Different Set Temperatures

It is assumed that the outdoor temperature remains constant, typically, with the upper limit of the set temperature being 26 °C to meet the thermal comfort requirements of consumers. By increasing the set temperature, the potential for the air conditioning clusters to participate in the demand response control is calculated. Taking the example of changing the set temperature from 23 °C to 24 °C, the temperature change of each room and the power variations of the air conditioning clusters are shown in Figure 7.

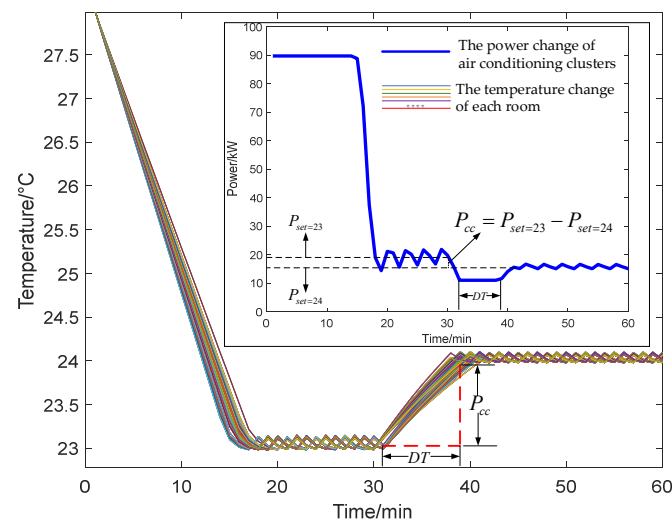


Figure 7. The temperature and power variations of the air conditioning clusters when the temperature is set from 23 °C to 24 °C.

In Figure 7, DT represents the time the air conditioning cluster maintains the minimum power after reaching it to raise the temperature indoors. The peak clipping capacity is defined as P_{cc} , representing the power of the air conditioning cluster at the set temperature, and the difference in power before and after participating in demand response. It can be expressed as $P_{cc} = P_{set2} - P_{set1}$.

The scenario is set with a set temperature of 23 °C as a reference, and the operating temperature of the air conditioning clusters is set from 23 °C to 24 °C, 25 °C, and 26 °C. The comparative results are presented in Table 3, analyzing the demand response potential of the air conditioning cluster.

Table 3. The results of the demand response capability of the air conditioning clusters.

Set Temperature	DT/min	P_{set}/kW	P_{CC}/kW	Power Reduction/%
Maintain at 23 °C	0	19.72	0	0
From 23 °C to 24 °C	7	16.67	3.05	15.4%
From 23 °C to 25 °C	16	14.39	5.33	27%
From 23 °C to 26 °C	31	11.24	8.48	43%

The results in Table 3 show that for every for every one-degree Celsius increase in the set temperature, the DT of the air conditioning cluster increases, and the degree of power reduction is around 14.4%.

6.2. The Resolution of the Control Strategy for the Variable-Frequency Air Conditioning Cluster

The existing variable-frequency air conditioning systems have already achieved a difference of 0.5 °C in the set temperature. In this case study, the initial temperature of each room is randomly set to 23 °C, or 23.5 °C, or 24 °C, and each air conditioning unit runs for 60 min. Figure 8a shows the temperature variation for each room, while Figure 8b shows

the power variation during the operation of each air conditioning unit. The different colors in the figures represent each air conditioning.

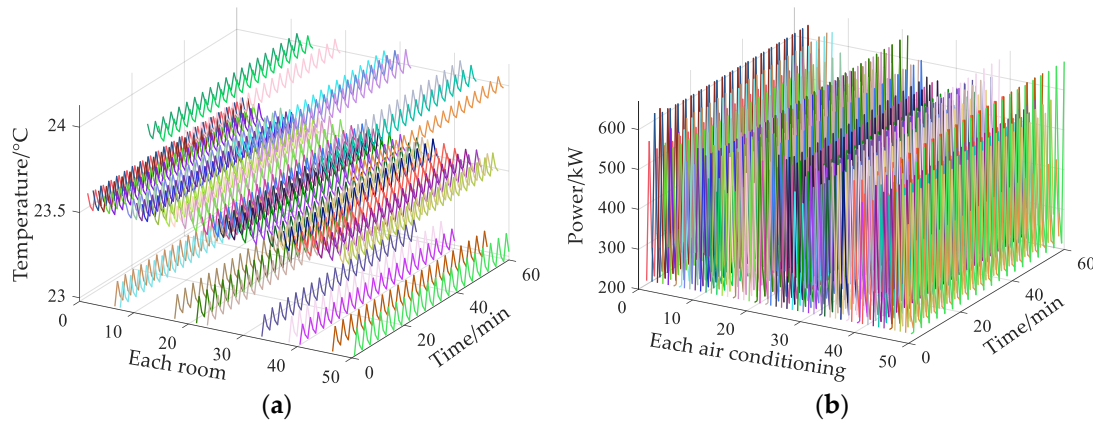


Figure 8. The state of the cluster of air conditioning unit running for 60 min. (a) The changes in temperature of each room. (b) The changes in power of each air conditioning unit.

Assuming the aggregator's day-ahead transaction volume ensures that the maximum power during the demand response period does not exceed 20 kW. The duration of demand response is 60 min. Each air conditioning unit adjusts its set temperature every 15 min, with four changes at 0, 15, 30, and 45 min.

Three scenarios are established to validate the precision of the MOPSO algorithm for the demand response control strategy proposed in this research:

Scenario 1: Only considering the accuracy of demand response;

Scenario 2: Only considering the thermal comfort of consumers;

Scenario 3: Simultaneously considering the accuracy of demand response and the thermal comfort of consumers.

In scenarios 1 and 2, the traditional PSO algorithm is used for optimization, while in scenario 3, the MOPSO algorithm is used for optimization.

6.2.1. Only Considering the Accuracy of Demand Response

For load aggregators, the accuracy of the demand response strategy holds significant importance. A low accuracy of demand response may affect the achievement of promised load reduction targets, potentially pulling down the reputations of the aggregator and the electricity market. Therefore, the accuracy of the demand response strategy is directly related to the income of the load aggregator.

The PSO algorithm is used to solve the function $o_1(t)$, and the results are shown in Figure 9.

After the control of the demand response strategy, the average temperature of 50 rooms increases to around 25 °C.

In Figure 10, the red curve represents the operational state of an air conditioning system before the control and the blue curve represents the operational state after the control. Before participating in the demand response control, the set temperature of this air conditioning unit is maintained at 23.5 °C. After the control, in the first 30 min, the set temperature of this air conditioning unit remains unchanged. At 30 min, the set temperature is changed to 24 °C, the power of this air conditioning unit decreases to the lowest operating power to cause the temperature of the room to rise to the set temperature, and the temperature of this room increases to a final value of 24 °C. Compared to the original operating state of this air conditioning unit, the load of the air conditioning system is reduced after the control.

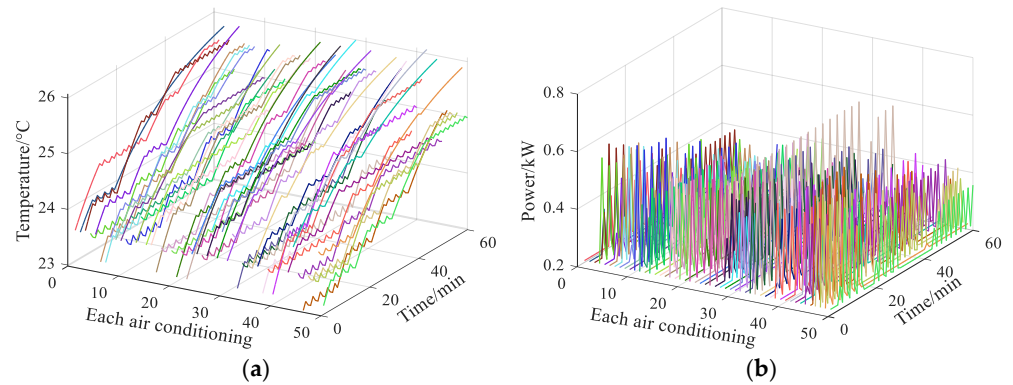


Figure 9. Scenario 1. (a) The changes in temperature of each room. (b) The changes in power of each air conditioning unit.

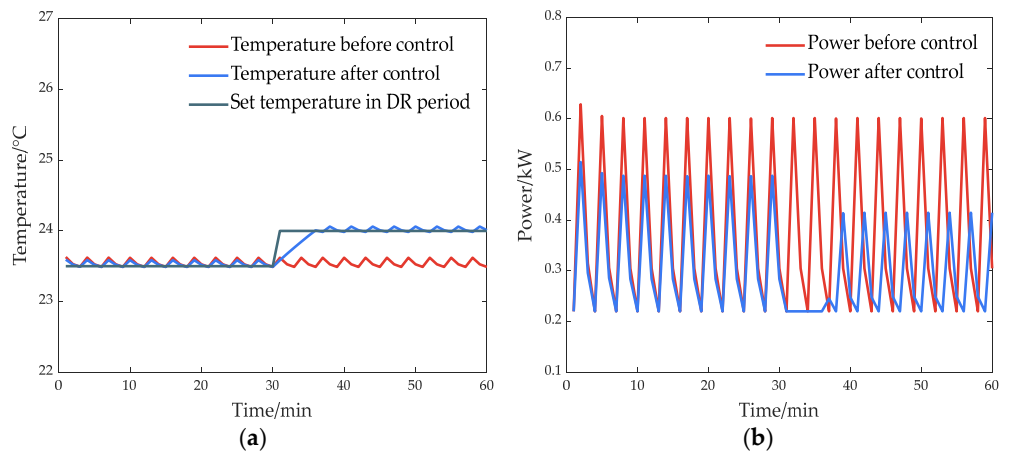


Figure 10. The operational state of an air conditioning unit in Scenario 1. (a) The change in temperature of the room. (b) The change in power of the air conditioning unit.

Figure 11 shows the instantaneous state of all air conditioning units at a certain moment during the demand response period in Scenario 1. After the control of demand response, the average temperature of 50 rooms is higher than the average temperature of 50 rooms before the control, and the power of each air conditioning unit after the control decreases compared to the power of each air conditioning unit before the control.

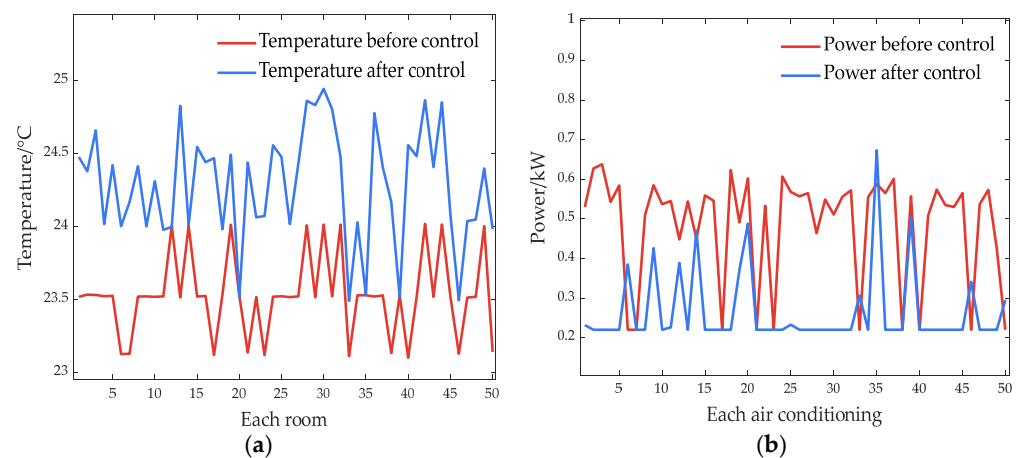


Figure 11. The instantaneous state of all air conditioning units at a certain moment in Scenario 1. (a) The changes in temperature of each room. (b) The changes in power of each air conditioning unit.

Figure 12 shows the total power variation of air conditioning clusters at each moment before and after the control of demand response in Scenario 1. The red curve represents the total power of air conditioning clusters before the control, while the blue curve represents the total power of air conditioning clusters after the control. The black curve represents the maximum allowed power during the demand response period. A single-objective optimization is performed to maximize the interests of the load aggregator, which meets the control requirements for demand response.

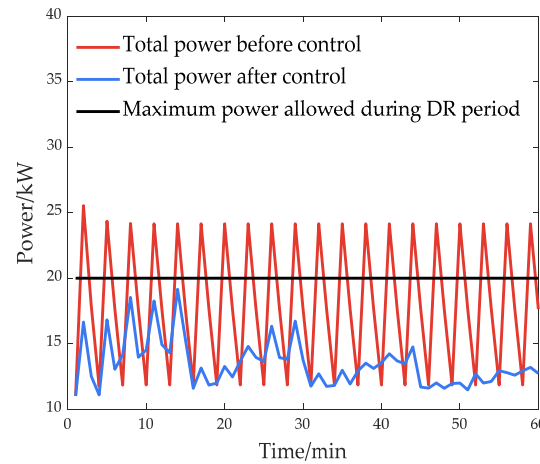


Figure 12. Comparison of total power of air conditioning clusters in Scenario 1.

In Scenario 1, the average temperature of the 50 rooms before the control is 23.5 °C, and after the control, it rises to 25.3 °C, with the highest temperature being 26.2 °C. The PMV value is 0.53, and the PPD value is 11%, indicating a slightly warm thermal sensation. However, it may not guarantee that the temperature of the rooms meets the requirements of human comfort. The air conditioning cluster is fully responsive.

6.2.2. Only Considering the Thermal Comfort of Consumers

For consumers, a warm and comfortable environment contributes to both physical health and psychological comfort. Extreme room temperatures, whether too high or too low, can lead to discomfort, affecting work efficiency of people. Therefore, in this scenario, the benefit for consumers is the demand for thermal comfort.

The PSO algorithm is used to solve the function $o_2(t)$, and the results are shown in Figure 13.

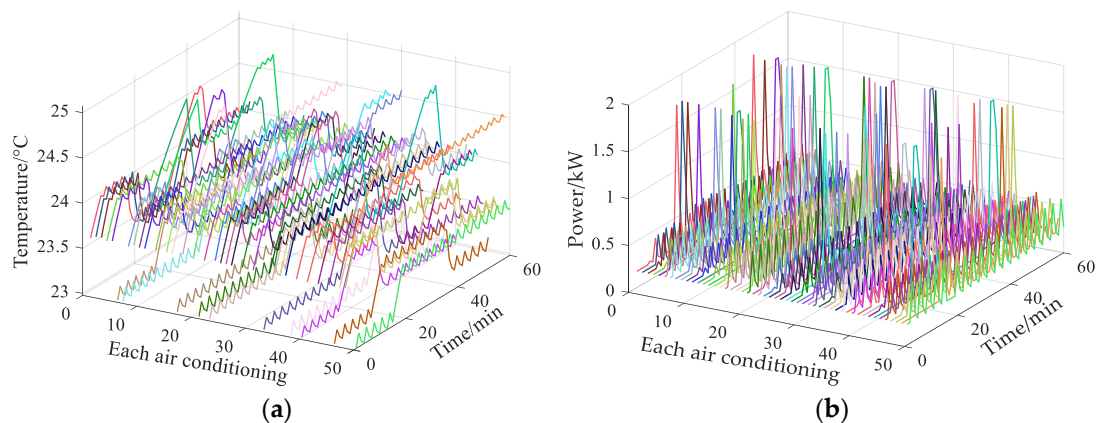


Figure 13. Scenario 2. (a) The changes in temperature of each room. (b) The changes in power of each air conditioning unit.

After the control of the demand response strategy, the average temperature increases to around 23.8 °C.

In Figure 14, the red curve represents the operational state of an air conditioning unit before the control and the blue curve represents the operational state after the control. Before participating in the demand response control, the set temperature of this air conditioning unit is maintained at 24 °C. After the control, in the first 15 min, the set temperature of this air conditioning unit is set to 25 °C. At 15 min, the set temperature is changed to 24 °C. At 30 min, the set temperature is changed to 24.5 °C. At 45 min, the set temperature returns to 24 °C, and the temperature of this room maintains a final value of 24 °C. In this case, there are two instances of full power operation during the DR period.

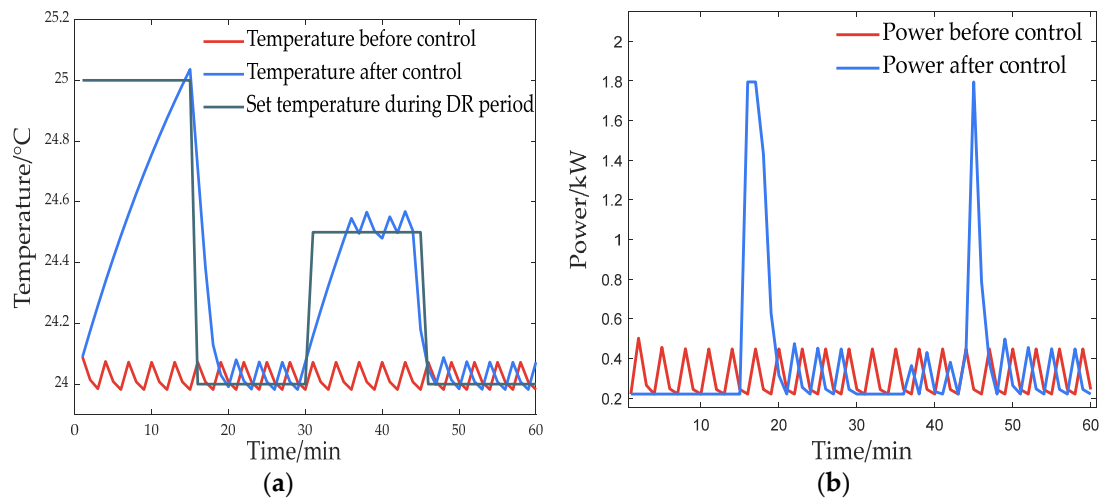


Figure 14. The operational state of an air conditioning unit in Scenario 2. (a) The changes in temperature of room. (b) The changes in power of each air conditioning unit.

The power after the control exhibits only a minor difference from the power before the control. Figure 15 shows the instantaneous state of all air conditioning units at a certain moment during the demand response period in Scenario 2. After the control of demand response, the average temperature of 50 rooms differs slightly from the average temperature of 50 rooms before the control, and the difference in power between each air conditioning unit after the control and before the control is relatively small.

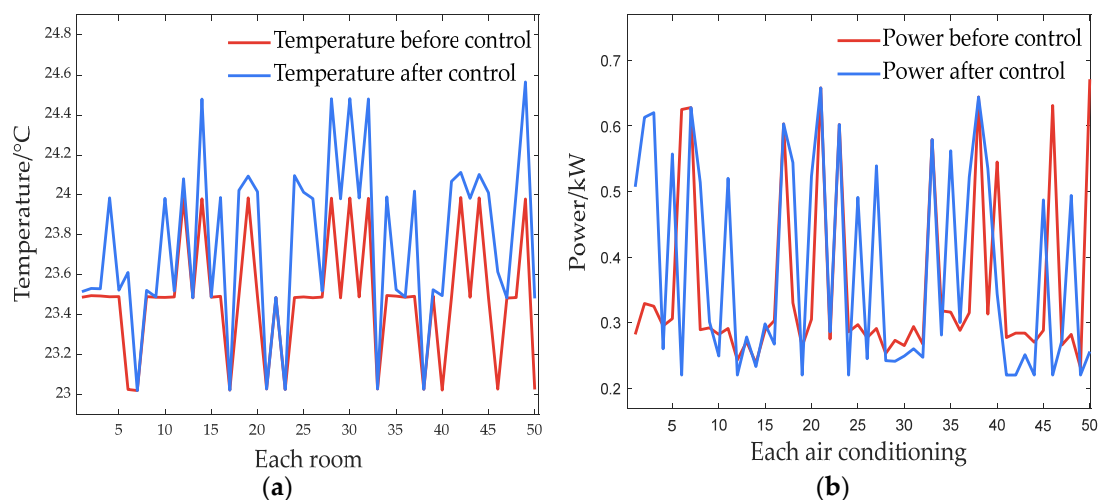


Figure 15. The instantaneous state of all air conditioning units at a certain moment in Scenario 2. (a) The changes in temperature of each room. (b) The changes in power of each air conditioning units.

Figure 16 shows that despite the optimization of consumer benefits as a single objective, the control results show minimal temperature variation, meeting the requirements for human comfort. However, the operating power exceeds the target maximum power, failing to meet the requirements for the demand response control.

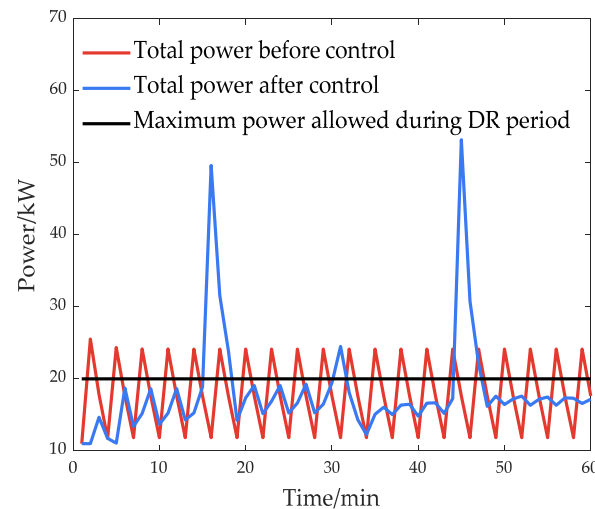


Figure 16. Comparison of total power of air conditioning clusters in Scenario 2.

In Scenario 2, the average temperature of 50 rooms before the control is 23.5 °C, and after the control, it increases to 23.8 °C. The highest temperature reaches 24.6 °C, with a PMV value of -0.05 , a PPD value of 5%, and a neutral thermal sensation, which ensures that the indoor temperature meets the requirements for human comfort. However, the accuracy of demand response in this scenario is 80%.

6.2.3. Simultaneously Considering the Accuracy of Demand Response and the Thermal Comfort of Consumers

The MOPSO algorithm is used to solve both function $o_1(t)$ and function $o_2(t)$, and the results are shown in Figure 17.

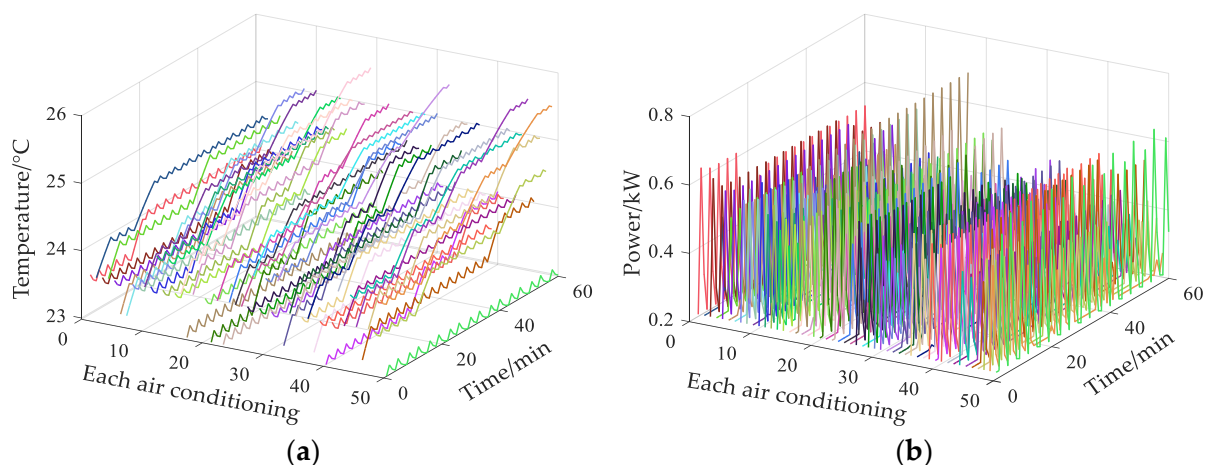


Figure 17. Scenario 3. (a) The changes in temperature of each room. (b) The changes in power of each air conditioning unit.

After the control of the demand response strategy, the average temperature increases to around 25.5 °C.

Figure 18 shows the total power variation of air conditioning clusters at each moment before and after the control of demand response in Scenario 3. After participating in the

demand response control, the set temperature of this air conditioning unit changed from 24 °C to 24.5 °C, and the power of this air conditioning unit decreases.

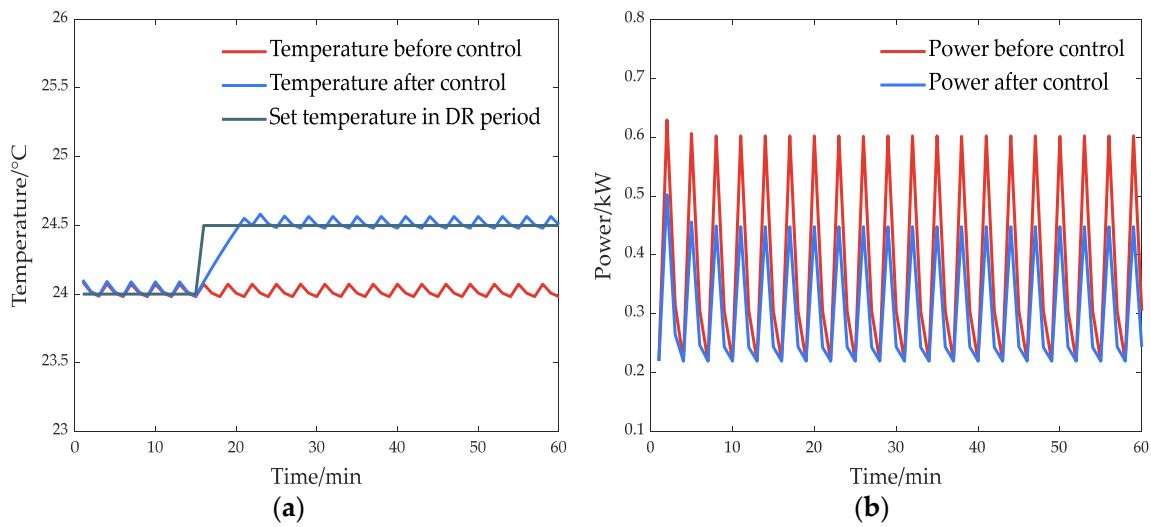


Figure 18. The operational state of an air conditioning unit in Scenario 3. (a) The changes in temperature of each room. (b) The changes in power of each air conditioning unit.

Figure 19 shows that at a certain moment during the demand response period, the power of all air conditioning systems is lower than the power before participating in the demand response, and the difference in temperature changes of room is within 1 °C.

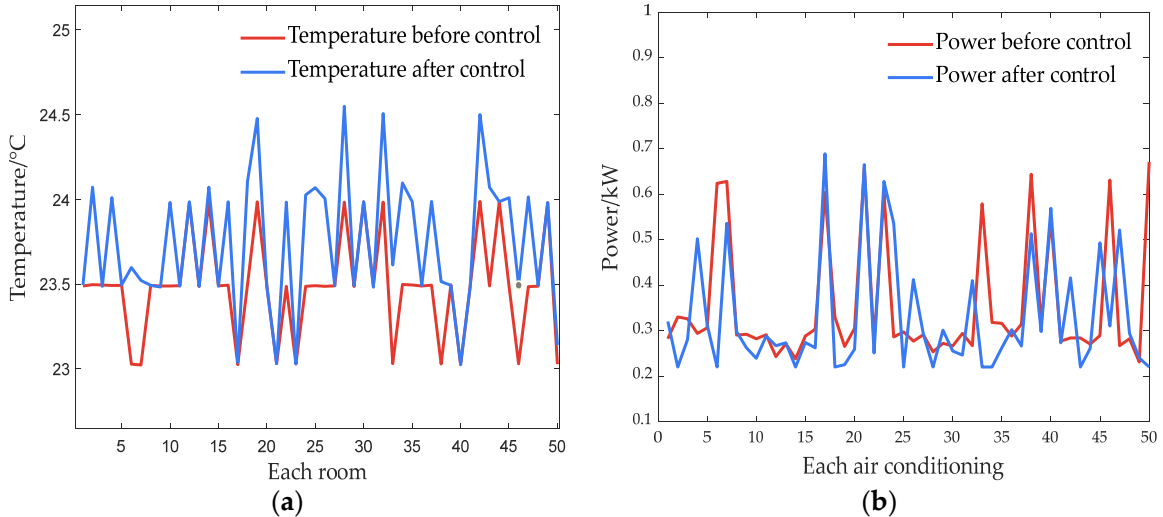


Figure 19. The instantaneous state of all air conditioning units at a certain moment in Scenario 3. (a) The changes in temperature of each room. (b) The changes in power of each air conditioning unit.

Figure 20 shows the results of using the MOPSO algorithm to solve a control strategy based on the accuracy of demand response and the thermal comfort of consumers. The results indicate minimal temperature variation, which meets human comfort requirements, and the power consumption satisfies the demands of the demand response control.

In Scenario 3, the lowest temperature after the control is 23.6 °C, with the PMV value is -0.13 , and the PPD value is 5%, a neutral thermal sensation. The highest temperature after the control reaches 25.5 °C, the PMV value is 0, of PPD value is 5%, and the thermal sensation is neutral. This indicates that the temperature after the control satisfies human comfort requirements. The air conditioning cluster is fully responsive.

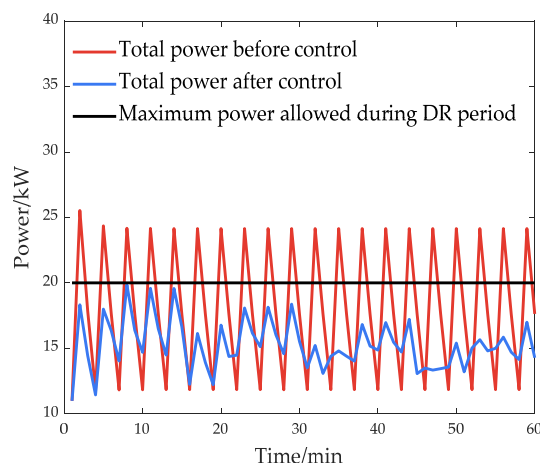


Figure 20. Comparison of total power of air conditioning clusters in Scenario 3.

6.3. Summary

The demand response control results for each scenario are shown in Table 4.

Table 4. The demand response control results for each scenario.

Scenario	The Minimum Temperature	The Maximum Temperature	PMV	PDD	Accuracy
1	23	26.2	[−0.34, 0.53]	[0, 11]	100%
2	23	24.6	[−0.34, −0.05]	[0, 5]	80%
3	23	25.5	[−0.34, 0.24]	[0, 5]	100%

In summary, the comprehensive analysis of the above scenarios indicates that the use of the MOPSO algorithm for the control strategy mentioned in this paper can simultaneously fulfill both the demand response of the load aggregator and the comfort requirements of consumers. This approach achieves a multi-objective control for the variable-frequency air conditioning cluster.

7. Conclusions

In summer, the rapid increase in air conditioning load leads to periodic adjustments in the power system, which results in insufficient peak capacity and places significant pressure on the electricity grid. This paper proposes a control strategy for building air conditioning cluster loads participating in demand response based on CPS architecture. The strategy effectively reduces the load of the air conditioning cluster during demand response to improve the operational safety of the power grid. Intelligent energy management, especially for high-consumption air conditioning systems, can substantially enhance energy efficiency and reduce operational costs, offering considerable economic benefits to commercial building managers. On another note, dynamically controlling air conditioning clusters based on real-time data and user demands, while ensuring human comfort, plays a crucial role in improving the satisfaction and experience of building occupants. The application and dissemination of such technologies serve as a model for energy management and environmental protection in smart city development, contributing to the overall advancement of urban intelligence.

The specific findings are summarized as follows:

(1) At the unit level of the CPS, an air conditioning load model based on the multiple parameter types of air conditioning compressors is proposed. By changing the values of the equivalent thermal capacitance and equivalent thermal resistance of each room, the simulation shows the operational states of the air conditioning system in different environments. This process validates the effectiveness of the load model of air conditioning clusters.

(2) At the system level of the CPS, the potential of air conditioning clusters to participate in demand response is analyzed by changing the set temperature of the air conditioning

cluster and analyzing the results. The result shows that for every one-degree Celsius increase in the set temperature, the time for air conditioning clusters to maintain minimum power will be extended, and the degree of power reduction is around 14.4%.

(3) At the SoS level of the CPS, a multi-objective optimization control strategy for air conditioning clusters is introduced. This model introduces a control function, which includes changing the set temperature of each air conditioning cluster every 15 min, ensuring that the total power after the control does not exceed the set value, and ensuring that the temperature of each room after the control can meet the demand of human thermal comfort. The overall objective of the control strategy is to achieve a high accuracy of demand response.

(4) An MOPSO algorithm based on the Pareto front is used to solve the multi-objective optimization of the control strategy. Three different scenarios were set up to compare the control strategy proposed in this paper. A traditional PSO algorithm is used for the single-objective solution of the first and the second scenes, and the MOPSO algorithm is used for the multi-objective solution of the third scene. The case study shows that compared to the PSO algorithm, the MOPSO optimization algorithm effectively searches and optimizes objectives, as well as providing decision-makers with the flexibility for decision-making and data optimization based on different preferences. The lowest temperature after the control is 23.6 °C, with the PMV value is −0.13, the PPD value is 5%, a neutral thermal sensation. The highest temperature after the control reaches 26 °C, the PMV value is 0.37, the PPD value is 8%, and the thermal sensation is neutral. This indicates that the temperature after the control satisfies human body comfort requirements. The DR control strategy achieves an accuracy rate of 92%. These findings demonstrate that the control strategy mentioned in this study is efficient in promoting power balance and stability in the power grid.

In summary, building air conditioning cluster load participation in demand response based on CPS architecture can effectively manage air conditioning energy consumption, convert air conditioning loads into flexible and controllable demand side resources, and effectively solve problems such as summer load surge, excessive air conditioning usage, and prominent peak loads.

Author Contributions: Conceptualization, X.Y.; Methodology, X.Y.; Software simulation, H.C.; Validation, H.L.; Formal analysis, H.C.; Investigation, J.X.; Resources, Z.C.; Data curation, Z.C. and H.L.; Writing—original draft, H.C.; Writing—review & editing, X.Y.; Visualization, H.C.; Supervision, X.Y.; Project administration, J.X. All authors have read and agreed to the published version of the manuscript.

Funding: This research received no external funding.

Data Availability Statement: Data are contained within the article.

Conflicts of Interest: The authors declare no conflict of interest.

References

1. Gao, C.; Li, Q.; Li, Y. Bi-level optimal dispatch and control strategy for air-conditioning load based on direct load control. *Proc. CSEE* **2014**, *34*, 1546–1555.
2. Wu, R.; Wang, D.; Xie, C.; Lai, C.S.; Huang, J.; Lai, L.L. Distributed Control Method for Air-conditioning Load Participating in Voltage Management of Distribution Network. *Autom. Electr. Power Syst.* **2021**, *45*, 215–222.
3. Gong, F.; Han, N.; Zhang, L.; Ruan, W. Analysis of Electricity Consumption Behavior of Air Conditioning based on the Perspective of Power Demand Response. In Proceedings of the 2020 IEEE International Conference on Advances in Electrical Engineering and Computer Applications (AEECA), Dalian, China, 25–27 August 2020; pp. 412–416.
4. Xu, Q.S.; Yang, C.X.; Yan, Q.G. Strategy of day-ahead power peak load shedding considering thermal equilibrium inertia of large-scale air conditioning loads. *Power Syst. Technol.* **2016**, *40*, 156–163.
5. Li, C.; Tian, P.; Wang, F. Energy saving control method research of modular water chillers group operation and pump variable-frequency control based on dynamic air conditioning load requirements analysis. In Proceedings of the 2010 International Conference on Computer, Mechatronics, Control and Electronic Engineering, Changchun, China, 24–26 August 2010; Volume 5, pp. 192–195.

6. Lu, N. An Evaluation of the HVAC Load Potential for Providing Load Balancing Service. *IEEE Trans. Smart Grid* **2012**, *3*, 1263–1270. [[CrossRef](#)]
7. Gao, S.; Wang, C.; Zhang, H.; Wang, Z.; Cheng, L.; Lin, Z. Research and Control Strategy of Air-conditioning Load Model Based on Demand Response. In Proceedings of the 2018 2nd IEEE Conference on Energy Internet and Energy System Integration (EI2), Beijing, China, 20–22 October 2018; pp. 1–5.
8. Wang, Y.; Tong, Y.; Huang, M.; Yang, L.; Zhao, H. Research on virtual energy storage model of air conditioning loads based on demand response. *Power Syst. Technol.* **2017**, *41*, 394–401.
9. Wang, D.; Fan, M.; Jia, H. Consumer consumers comfort constraint demand response for residential thermostatically-controlled loads and efficient power plant modeling. *Proc. CSEE* **2014**, *34*, 2071–2077.
10. Rao, D.V.; Ukil, A. Modeling of Room Temperature Dynamics for Efficient Building Energy Management. *IEEE Trans. Syst.* **2020**, *50*, 717–725. [[CrossRef](#)]
11. Zhang, W.; Lian, J.; Chang, C.-Y.; Kalsi, K. Aggregated modeling and control of air conditioning loads for demand response. In Proceedings of the 2014 IEEE PES General Meeting Conference & Exposition, National Harbor, MD, USA, 27–31 July 2014; p. 1.
12. Bashash, S.; Fathy, H.K. Modeling and Control of Aggregate Air Conditioning Loads for Robust Renewable Power Management. *IEEE Trans. Control. Syst. Technol.* **2013**, *21*, 1318–1327. [[CrossRef](#)]
13. Yao, L.; Lu, H.-R. A Two-Way Direct Control of Central Air-Conditioning Load Via the Internet. *IEEE Trans. Power Deliv.* **2009**, *24*, 240–248. [[CrossRef](#)]
14. Song, M.; Ciwei, G.; Yang, J.; Liu, Y.; Cui, G. Novel Aggregate Control Model of Air Conditioning Loads for Fast Regulation Service. *IET Gener. Transm. Distrib.* **2017**, *11*, 4391–4401. [[CrossRef](#)]
15. Chen, L.; Wan, Y.; Zhang, F.; Wang, X.; Wang, Y. Operation mode and control strategy for air-conditioning service based on business of load aggregator. *Autom. Electr. Power Syst.* **2018**, *42*, 8–18.
16. Jiang, T.; Jv, P.; Wang, C. Aggregated Power Model of Air-conditioning Load Considering Stochastic Adjustment Behaviors of Consumers. *Autom. Electr. Power Syst.* **2020**, *44*, 105–113.
17. Wang, Y.; Zhang, P.; Yao, Y. Cyber-physical modeling and control method for aggregating large-scale ACLs. *Proc. CSEE* **2019**, *39*, 6509–6521.
18. Tian, A.; Li, W.; Liu, D.; An, T.; Li, D.; Gao, D. Control Strategy of Air Conditioning Load Based on Improved State-space Mode. *Autom. Electr. Power Syst.* **2019**, *43*, 124–130.
19. Dagdougui, H.; Minciardi, R.; Ouammi, A.; Robba, M.; Sacile, R. Modeling and optimization of a hybrid system for the energy supply of a “Green” building. *Energy Convers. Manag.* **2012**, *64*, 351–363. [[CrossRef](#)]
20. Joe, J.; Karava, P. A model predictive control strategy to optimize the performance of radiant floor heating and cooling systems in office buildings. *Appl. Energy* **2019**, *245*, 65–77. [[CrossRef](#)]
21. Vedullapalli, D.T.; Hadidi, R.; Schroeder, B. Combined HVAC and Battery Scheduling for Demand Response in a Building. *IEEE Trans. Ind. Appl.* **2019**, *55*, 7008–7014. [[CrossRef](#)]
22. Li, N.; Cheung, S.C.; Li, X.; Tu, J. Multi-objective optimization of HVAC system using NSPSO and Kriging algorithms—A case study. *Build. Simul.* **2017**, *10*, 769–781. [[CrossRef](#)]
23. Lin, C.J.; Wang, K.J.; Dagne, T.B.; Woldegiorgis, B.H. Balancing thermal comfort and energy conservation— A multi-objective optimization model for controlling air-condition and mechanical ventilation systems. *Build Environ.* **2022**, *219*, 109237. [[CrossRef](#)]
24. Yang, S.; Yu, J.; Gao, Z.; Zhao, A. Energy-saving optimization of air-conditioning water system based on data-driven and improved parallel artificial immune system algorithm. *Energy Convers. Manag.* **2023**, *283*, 116902. [[CrossRef](#)]
25. Cintuglu, M.H.; Mohammed, O.A.; Akkaya, K.; Uluagac, A.S. A Survey on Smart Grid Cyber-Physical System Testbeds. *IEEE Commun. Surv. Tutor.* **2017**, *19*, 446–464. [[CrossRef](#)]
26. Borth, M.; Verriet, J.; Muller, G. Digital Twin Strategies for SoS 4 Challenges and 4 Architecture Setups for Digital Twins of SoS. In Proceedings of the 2019 14th Annual Conference System of Systems Engineering (SoSE), Anchorage, AK, USA, 19–22 May 2019; pp. 164–169.
27. Yang, Z.; Ding, X.; Lu, X.; Jing, J.; Gao, C. Inverter air conditioning load modeling and operational control for demand response. *Power Syst. Prot. Control.* **2021**, *49*, 132–140.
28. Ou, M.; Chen, Z.; Tan, W.; Wen, M.; Zhou, Z. Optimization of electric vehicle charging load based on peak-to-valley time-of-use electricity price. *Power Syst. Prot. Control.* **2020**, *35*, 54–59.
29. Sun, Z.; Sun, J.; Zhao, M.; Chen, Y. Analysis of thermal comfort in aircraft cockpit based on the modified PMV index. *Acta Aeronaut. Astronaut. Sin.* **2015**, *36*, 819–826.
30. Sarbu, I.; Pacurar, C. Experimental and numerical research to assess indoor environment quality and schoolwork performance in university classrooms. *Build. Environ.* **2015**, *93*, 141–154. [[CrossRef](#)]
31. Coello, C.C.; Lechuga, M.S. MOPSO: A proposal for multiple objective particle swarm optimization. In Proceedings of the 2002 Congress on Evolutionary Computation, Honolulu, HI, USA, 12–17 May 2002; pp. 1051–1056.

Disclaimer/Publisher’s Note: The statements, opinions and data contained in all publications are solely those of the individual author(s) and contributor(s) and not of MDPI and/or the editor(s). MDPI and/or the editor(s) disclaim responsibility for any injury to people or property resulting from any ideas, methods, instructions or products referred to in the content.